

Tracing the sources of cosmic rays with molecular ions

Julia K. Becker

*Ruhr-Universität Bochum, Fakultät für Physik & Astronomie, Theoretische Physik IV, D-44780
Bochum, Germany*

julia@tp4.rub.de

John H. Black

*Dept. of Earth and Space Sciences, Chalmers University of Technology, Onsala Space
Observatory, SE-439 92 Onsala, Sweden*

Mohammadtaher Safarzadeh¹

*Dept. of Earth and Space Sciences, Chalmers University of Technology, Onsala Space
Observatory, SE-439 92 Onsala, Sweden*

Florian Schuppan

*Ruhr-Universität Bochum, Fakultät für Physik & Astronomie, Theoretische Physik IV, D-44780
Bochum, Germany*

ABSTRACT

The rate of ionization by cosmic rays in interstellar gas directly associated with γ -ray emitting supernova remnants is for the first time calculated to be several orders of magnitude larger than the Galactic average. Analysis of ionization-induced chemistry yields the first quantitative prediction of the astrophysical H_2^+ emission line spectrum, which should be detectable together with H_3^+ lines. The predicted coincident observation of those emission lines and γ -rays will help prove that supernova remnants are sources of cosmic rays.

Subject headings: supernovae: general — cosmic rays — acceleration of particles — stars: winds, outflows — shock waves — radio continuum: general

1. Introduction

One of the central questions in modern physics concerns the origin of cosmic rays (CRs). The CRs themselves do not directly reveal their sources as they interact with cosmic magnetic fields

¹*Now at:* Dept. of Physics and Astronomy, Johns Hopkins University, 3400 N. Charles Street Baltimore, MD 21218, USA

and particles on their way through the Universe (Strong et al. 2007). One method of identifying CR sources indirectly is the search for high-energy photon or neutrino signals. When protons of energy $E > 200$ MeV interact with photon or matter fields in the vicinity of the CR production site, charged and neutral pions are produced, which then emit high-energy neutrinos and photons. Those neutral particles can be used to trace CRs, as they point back to the sources. This approach is limited by (a) the low interaction cross sections that make neutrinos difficult to detect (Becker 2008), and (b) the competition with processes like inverse Compton scattering and bremsstrahlung (Schlickeiser 2002). It is therefore crucial to use multiwavelength approaches to identify CR sources through correlation studies, and not to rely solely on the observation of high-energy photons.

The illumination of molecular clouds by CRs from supernova remnants (SNRs) was first suggested by Black and Fazio (1973); Montmerle (1979). Most recently, observations performed with the Fermi Telescope have revealed high-energy emission from several regions associated with a SNR located in close proximity to molecular clouds (MCs). In particular, emission at 0.2 to 200 GeV has been detected towards the SNRs W51C (Abdo et al. 2009), W28 (Abdo et al. 2010a), W44 (Abdo et al. 2010b), W49B (Abdo et al. 2010c) and IC443 (Abdo et al. 2010d). SNRs are one of the primary candidates for CR acceleration, as discussed for example by Biermann et al. (2009). The observed gamma-ray signatures could therefore be interpreted as π^0 -decay products from high-energy CR interactions with the MC. The data for these particular objects actually seem to favor a hadronic scenario over a leptonic one, see e.g. (Abdo et al. 2010b). Due to the ambiguity of the signal, however, other tracers of CRs are needed to have a final proof.

In this paper, we quantify a new method to identify SNRs as CR sources, based on CR-induced ionization. When CRs are accelerated in a SNR and then injected into a nearby MC, the ionization rate in the ambient gas is expected to be enhanced compared with the ionization caused by the general background of Galactic CRs. The immediate products are hydrogen ions, H^+ and H_2^+ , which react rapidly with H_2 and oxygen to form molecular ions. Ions like H_3^+ , OH^+ , H_2O^+ , and H_3O^+ are spectroscopically observable at infrared and submm wavelengths and their abundances are predictable as functions of the ionization rate (e.g. (Black 1998; Montmerle 2009)). Among the 18 molecular cations now identified in the interstellar medium, it is the reactive ions H_3^+ , OH^+ , and H_2O^+ that are expected to be the most specific tracers of the CR ionization rate (Black 1998, 2007), and it was only during the last year that the latter two species have been detected (Benz et al. 2010; Bruderer et al. 2010; Gerin et al. 2010; Gupta et al. 2010; Krelowski et al. 2010; Neufeld et al. 2010a; Ossenkopf et al. 2010; Schilke et al. 2010; Wyrowski et al. 2010). Analysis of OH^+ and H_2O^+ absorption in diffuse interstellar gas of low molecular fraction ($H_2/H < 10\%$) serves to calibrate the background ionizing frequency of interstellar hydrogen at a level $\zeta_{Gal} = (0.6 - 2.4) \cdot 10^{-16} s^{-1}$ per atom (Gerin et al. 2010; Neufeld et al. 2010a,b).

2. Ionization in the direct vicinity of supernova remnants

Here, we estimate the enhanced interstellar ionization rates expected from the observed fluxes of high-energy gamma rays toward SNRs and predict the abundances of reactive molecular ions to be expected in associated MCs. We show how correlations between GeV-TeV emission and vibrational and rotational spectra of molecular ions could be used to identify the sites of CR acceleration. Observational tests will be possible through astronomical spectroscopy at infrared and mm/submm wavelengths. CRs of kinetic energies between $E_p \sim 1$ MeV and ~ 1 GeV ionize the interstellar medium, while those at lower energy hardly escape their sources. We investigate five SNRs located in or close to MCs, which are detected in gamma-rays.

2.1. Primary particle spectra

The CR spectra, further used to calculate the ionization rate, can be deduced from the measured gamma-ray flux at Earth:

$$\frac{dN_\gamma}{dE_\gamma dt dA_{Earth}}. \quad (1)$$

Assuming that the photons arise from hadronic interactions between the SNR and the MC, a primary CR spectrum can be derived. We assume a smoothed broken power-law for the primaries:

$$\frac{dN_p}{dE_p dt dA_{source}} = a_p \left(\frac{p}{1 \text{ GeV } c^{-1}} \right)^{-s} \left(1 + \left(\frac{p}{p_{br}} \right) \right)^{-\Delta s}, \quad (2)$$

where a_p is the proton spectrum normalization and p_{br} the location of the spectral break. For all sources, this shape of the primary spectrum reproduces the shape of the observed photon spectrum. Our results generally follow the original calculations by Fermi, (Abdo et al. 2009, 2010a,b,c,d) with slight modifications of the smoothing of the power-law, only giving minor changes to the result.

We use the parametrization of the CR interaction model as presented in Kamae et al. (2006) to derive the primary spectrum from the gamma-ray observation. We use a fixed value of the hydrogen density, $n_H = 100 \text{ cm}^{-3}$ and determine the CR energy W_p needed to provide the observed gamma-ray flux. The volume of the emitting region V enters the normalization of the proton spectrum. It can be derived from gamma-observations and is taken from the Fermi publications. The spectral parameters s , Δs and p_{br} , the total energy budget of interacting protons, W_p and the volume V are listed in Table 1.

2.2. Ionization

To calculate the ionization rate, we use the parametrization from Padovani et al. (2009), including ionization by CR electrons, CR protons and electron capture by CR protons. Only the

	W51C	W44	W28	IC443	W49B
s	1.5	1.74	1.7	2.09	2.0
Δs	1.4	1.96	1.0	0.78	1.4
p_{br} [GeV c ⁻¹]	15	9	2	69	4
W_p [10 ⁴⁹ erg]	9.0	12.1	3.3	28.0	35.0
V [cm ³]	$3.3 \cdot 10^{60}$	$4.2 \cdot 10^{59}$	$3.2 \cdot 10^{59}$	$4.2 \cdot 10^{59}$	$6.3 \cdot 10^{56}$

Table 1: Parameters used to derive the primary cosmic ray spectrum from the observed photon spectrum. The total energy budget of the sources and the spectral shape are determined from the observed gamma-ray spectrum, the interacting volume is deduced from the emitting region (see the original Fermi papers).

direct ionization by primary protons turns out to be significant, the other contributions being at least one order of magnitude smaller. The ionization rate of H₂ by primary protons reduces to

$$\zeta^{H_2} = \int_{E_{\min}}^{E_{\max}} \frac{dN_p}{dE_p} \sigma_p^{\text{ion}}(E_p) dE_p, \quad (3)$$

with dN_p/dE_p as the CR spectrum at a given kinetic energy E_p . The upper integration limit is set to $E_{\max} = 1$ GeV, as the rapidly decreasing cross section makes contributions at higher energies negligible.

There are two main factors affecting the ionization rate:

- (1) The CR spectrum at Earth as measured below ~ 1 GeV is modified from the spectrum at the source by transport effects of the ISM and the solar environment. The particle spectrum at the source can be derived from gamma-ray data up to approximately 1 GeV, but it must be estimated theoretically at lower energies. The simplest approach is to extrapolate the spectrum towards lower energies, assuming that the acceleration mechanism works the same way at MeV energies. However, low-energy particles might follow a different acceleration scheme and produce a flatter or curved spectrum, see Blasi et al. (2005) and references therein. This might lead to an overestimation of the spectrum at the lowest energies. However, it is not clear yet at what energy this will start exactly.
- (2) The choice of lower energy threshold E_{\min} is related to propagation effects. The range of a 1 MeV proton in hydrogen is 8.5×10^{-4} g cm⁻², which corresponds to a projected column density of 5.1×10^{20} H cm⁻². This is easily able to support detectable abundances of OH⁺ and H₂O⁺ in the diffuse molecular gas of the Galaxy. In Indriolo et al. (2009), a threshold of $E_{\min} = 2$ MeV is recommended for diffuse clouds with hydrogen number densities $n_H < 10^3$ cm⁻³, and $E_{\min} = 10$ MeV for dense clouds, where $n_H > 10^3$ cm⁻³. Close to a CR accelerator, at an average density of 100 cm⁻³, values above 2 MeV are reasonable choices to account for the stopping range.

We chose the following approach to account for these uncertainties: we first assume that the spectrum continues as a power-law down to MeV energies. We then introduce an artificial and sharp cutoff in the spectrum at a minimum kinetic energy E_{\min} , below which the CR flux is set to zero. We then vary the minimum energy between $E_{\min} = 1$ MeV and 100 MeV. As the CR ionization cross section decreases with energy, increasing the threshold will remove much of the potential signal, having an even more extreme effect than flattening the CR spectrum. Increasing the threshold at the same time accounts for considering different stopping ranges. At this stage, due to the lack of knowledge of the lower part of the spectrum, we will calculate the possible range of ionization intensity rather than one specific value.

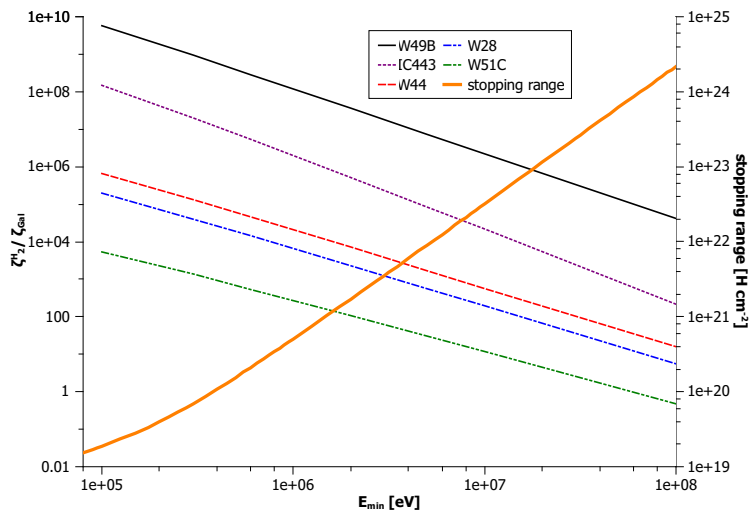


Fig. 1.— Dependence of the ionization rate, normalized to the average Galactic value of $\zeta_{\text{Gal}} := 2 \cdot 10^{-16} \text{ s}^{-1}$, on E_{\min} .

Figure 1 shows the ionization rate, normalized to Galactic average, versus the minimum energy. For comparison, the stopping range is shown as a function of E_{\min} . For the most optimistic scenario, still compatible with current knowledge, $E_{\min} = 2$ MeV, ionization rates range from 110 to $4 \cdot 10^7$ times the Galactic average. An energy cutoff at 100 MeV leaves W49B as an outstanding source with a factor of $4 \cdot 10^4$ above Galactic average. The central reason is the large CR energy density in this source (Abdo et al. 2010c). At $E_{\min} = 100$ MeV, only W51C drops to values below ζ_{Gal} . All other sources remain a factor of a few to ten above the background.

Note that we do not include the additional ionization by energetic secondary electrons being produced in the primary ionizing event. These secondary ionizations increase the total rate by factors of a few (cf. Padovani et al. 2009), but the details are sensitive to the relative abundances of H, H₂, e⁻, and He (Dalgarno et al. 1999). The escape of CRs from their sources and their propagation into surrounding material are also affected in complicated ways by interaction with magnetic fields (see Padovani and Galli (2011) for a recent discussion for dense molecular gas). These issues will be addressed in future work.

3. Cosmic ray induced molecular ions

As shown below, the observable line intensities of molecular ions spawned by CR ionization depend upon the ionization rate integrated through a column of molecular gas

$$\eta = \int_0^L \zeta^{\text{H}_2} n(\text{H}_2) dl \approx \zeta^{\text{H}_2} n(\text{H}_2) L \text{ s}^{-1} \text{ cm}^{-2},$$

which we call the *cosmic ray exposure*. The number density of interstellar H_2 is $n(\text{H}_2)$ and the integration is over path length $\ell = 0$ to L . Because the CRs of shortest range die off at small ℓ , protons at energies significantly greater than E_{min} contribute to the exposure. In principle, the exposure should be computed through an explicit depth-integration of the discrete energy loss. The SNRs discussed in this context have a CR exposure of the order of $\eta \sim 10^9 \text{ s}^{-1} \text{ cm}^{-2}$ or higher (see Fig. 1), which is $> 10^4$ times larger than the exposures that characterize diffuse clouds in the Galactic disk. In general, ionization by X-rays can produce similar chemical signatures. We expect the X-rays from SNRs to be much less important than CRs because the X-ray luminosities are relatively small and their depths of penetration are too short to yield high values of the exposure.

The outlines of interstellar ion chemistry have been understood for almost 40 years (Herbst and Klemperer 1973) and the rate coefficients of all the crucial reactions are well determined. In steady state between the rates of source and sink reactions, the number densities of the transient ions O^+ , OH^+ , H_2O^+ , and HeH^+ are expected to be proportional to ζ_{H} . In fully molecular regions, $n(\text{H}) \ll n(\text{H}_2)$, of low ionization $x(e^-) < 10^{-5}$, competing processes rarely interrupt the sequence of H-atom abstraction reactions so that almost every ionization of hydrogen leads to formation of H_2^+ , H_3^+ , OH^+ , H_2O^+ , and H_3O^+ . The time-scales to achieve steady state are very short, $\sim 1(1000 \text{ cm}^{-3}/n(\text{H}_2))$ year.

The abundances of interstellar molecules can be computed from a system of rate equations for various values of the physical conditions (density, temperature, ionization rate) and gas-phase elemental abundances, either in the steady-state limit or as a time-dependent solution. However, the abundances alone do not characterize observable signatures, because the distributions of the molecules among their quantum states tend to be far out of equilibrium. The departures from equilibrium will be most extreme for the most reactive molecular ions, because elastic and inelastic collisions that would otherwise thermalize them are typically not faster than the reactive collisions with the main collision partner, H_2 , that destroy them (Black 1998). We illustrate the coupled effects of ion chemistry and non-equilibrium excitation with results from a reference model of molecular gas at density $n(\text{H}_2) = 100 \text{ cm}^{-3}$ exposed to an ionization rate $\zeta^{\text{H}_2} = 10^{-12} \text{ s}^{-1}$ over a path length $L = 10^{19} \text{ cm} = 3.24 \text{ pc}$. The excitation and transport of spectrum lines are computed through use of the `Radex` program, which can incorporate formation and destruction rates state-by-state for reactive molecules along with all relevant radiative and inelastic collision processes (van der Tak et al. 2007). The kinetic temperature of the molecular gas is assumed to be 150 K, somewhat elevated owing to enhanced heating by cosmic rays. All line widths are taken to be 9.394 km s^{-1} . Full details of these calculations will be presented elsewhere. Because H_2^+ has

no permanent dipole moment, its vibration-rotation and pure rotational spectrum occurs only as weak electric quadrupole transitions. Upon birth by ionization of H_2 , H_2^+ is endowed with high vibrational excitation but it retains the relatively cold rotational distribution of its parent. At gas densities below 10^4 cm^{-3} , excited H_2^+ decays to the ground state by radiation more rapidly than it is destroyed or excited by collisions. As a result, the emitted spectrum in our reference model is directly predictable from the value of the CR exposure, $\eta = 10^9 \text{ s}^{-1} \text{ cm}^{-2}$, and the known quadrupole transition probabilities (Posen et al. 1983). Owing to symmetry-breaking in the last few bound vibration-rotation levels near the dissociation limit, H_2^+ exhibits a few dipole-allowed radio-frequency transitions (Brown and Carrington 2003; Howells and Kennedy 1991; Moss 1993; Bunker and Moss 2000; Critchley et al. 2001). These transitions are excited in our model by the small fraction of ionizations that put H_2^+ into levels ($v = 19, J = 0, 1$) of the $1s\sigma_g$ ground electronic state. Transitions to three barely bound levels ($v = 0, J = 0, 1, 2$) of the $2p\sigma_u$ state occur with high probabilities (Moss 1993) that partly compensate for the low populations of the initial states: we predict that these transitions at 17.6, 52.9, and 96.4 GHz will appear as weak masers in regions of high CR exposure. The electronically excited levels also radiate rapidly to $1s\sigma_g(v = 17 - 18, J = 0 - 3)$ in transitions at mm/submm wavelengths. Although these symmetry-breaking transitions will probably be undetectably weak in sources like those considered here, they may become observable in the more extreme environments in active galactic nuclei.

The high excitation of H_2^+ is partly transferred to H_3^+ in the next chemical step and H_3^+ can also be excited by collisions several times during its lifetime. The distortion-induced rotational transition (Pan and Oka 1986) of H_3^+ ($J, K = 4, 4 \rightarrow 3, 1$) easily suffers population inversion (Black 1998), a necessary condition for a maser. The transition frequency is poorly known (approximately 217.7 GHz), but the line is predicted in our reference model to appear as a weak maser with a peak Rayleigh-Jeans brightness temperature of 10 mK, an intensity that is detectable with existing radio telescopes. The intrinsically weak, far-infrared rotational transitions of H_3^+ are excited mainly by collisions at the kinetic temperature of the gas, while the infrared vibration-rotation transitions of both H_2^+ and H_3^+ are excited in the formation process with superthermal intensity distributions. In general, the rotational line intensities of H_3^+ will depend upon the local density and temperature; however, the entire spectrum of H_2^+ is rather insensitive to these physical conditions. We calculate explicitly the formation rate of HeH^+ by vibrationally excited H_2^+ and predict the spectrum that results from its initial, superthermal excitation. The predicted spectra are illustrated in Figure 2. At infrared wavelengths the strongest lines of H_3^+ appear between 3 and 4.6 μm while H_2^+ lines of comparable intensity appear between 4 and 6 μm . The strongest vibration-rotation lines of HeH^+ in this region are several hundred times weaker. In the far-infrared region, the thermally excited lines of H_3^+ are quite strong while the lines of HeH^+ are again considerably weaker. In the far-infrared, thermal emission by interstellar dust particles will produce continuous radiation with typical surface brightness $\geq 0.1 \text{ Jy nsr}^{-1}$ at a wavelength of 100 μm ; even so, it appears that the strongest rotational lines of H_3^+ might be observable if the spectroscopic resolving power is at least 100 (resolution of 1 μm at 100 μm wavelength). For comparison, the weak H_3^+ feature at 30.725 μm has an intensity approximately 1/2 as large as that of the H_2 $J = 2 \rightarrow 0$ line at

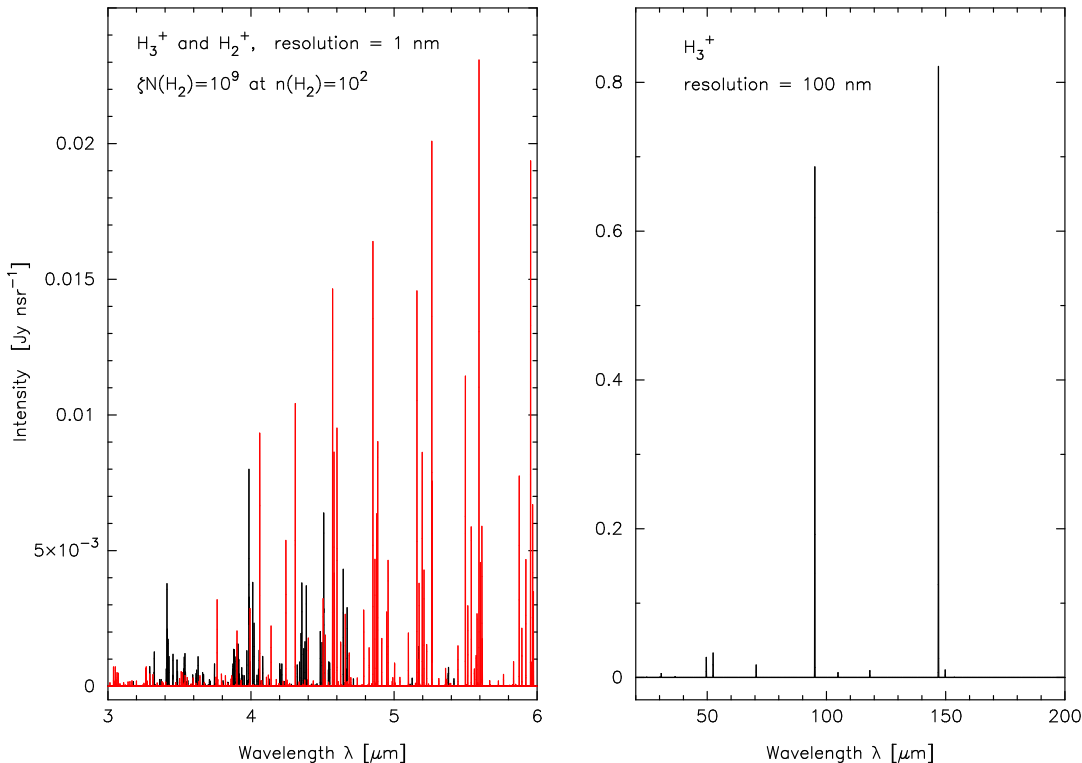


Fig. 2.— Predicted emission spectra of H_2^+ (red in online version) and H_3^+ (black online) for the reference model. The surface brightness is displayed in Jy nsr^{-1} where $1 \text{ Jy} = 10^{-26} \text{ W m}^{-2} \text{ Hz}^{-1}$ and $1 \text{ nsr} = 10^{-9}$ steradian of solid angle. In the figure, $\eta = 10^9 \text{ s}^{-1} \text{ cm}^{-2}$ is used as a typical value in this context (see text).

28.226 μm . We have also calculated the spectra of the OH_n^+ ions, $n = 1 - 3$. These ions form mainly as a result of reactions of thermalized H_3^+ or H^+ with oxygen and subsequent reactions with H_2 . The excess energy (enthalpies of reactants minus products) of each reaction will go partly into vibrational and rotational excitation of the product, so that the OH_n^+ ions will also exhibit superthermal excitation. A predicted signal of enhanced production of oxygen-bearing ions will be strong absorption in rotation-inversion transitions arising in highly metastable states of H_3O^+ at frequencies 1.6 to 1.9 THz. Absorption spectroscopy of interstellar H_3^+ has already suggested enhanced rates of ionization throughout the central molecular zone of the Galaxy (Goto et al. 2008; Geballe and Oka 2010) and in two locations near the SNR IC 443 (Indriolo et al. 2010a). We predict that emission lines of both H_2^+ and H_3^+ will be detectable and that their intensities can be used to measure the CR exposure.

4. Summary

We have calculated the associated cosmic ray ionization rate in interstellar matter near SNRs. While the exact value will depend on the exact density and spectral shape, we expect ionization to be significantly above Galactic average. The cosmic ray exposure of the interstellar hydrogen (ionization rate times gas density integrated over path length) for the SNRs W51C, W28, W44, IC443 and W49B is expected to be of the order of $\eta = 10^9 \text{ s}^{-1} \text{ cm}^{-2}$. This permits the construction of a coupled model of the ion chemistry and the excitation of reactive molecular ions that might serve as specific tracers of cosmic rays near their sources. Predictions are made of the intensities of rotational and vibration-rotation transitions of the reactive ions including the first quantitative prediction of an astronomical spectrum of H_2^+ . It appears that superthermally excited emission lines of H_2^+ and H_3^+ may be detectable at wavelengths between 3 and 6 μm . Strong thermal emission of H_3^+ may be measurable in the far infrared at 50 to 150 μm wavelength. W49B seems to be an outstanding candidate for the detection, with predicted ionization rate more than 4 orders of magnitude above Galactic average. Future measurements by e.g. Herschel and ALMA provide the opportunity to make observations of ionization signatures in SNR/MC systems and analyze their correlation to the gamma-ray emission. A recent observation suggests an enhanced excitation and abundance of ammonia toward W28 (Nicholas et al. 2011). Using *Radex*, it is possible to explain the observed spectrum as CR induced with an ionization rate of $4.5 \cdot 10^{-12} \text{ s}^{-1}$, so a factor of $> 10^4$ above Galactic average. Further, H_3^+ emission observed from the direction of IC443 indicates an enhanced ionization level of $2 \cdot 10^{-15} \text{ s}^{-1}$, so a factor of 10 above Galactic average (Indriolo et al. 2010b). In the future, more observations need to be performed in order to explicitly search for the expected signatures of H_2^+ and H_3^+ . Treating the propagation of the CRs in detail will allow us to give even more precise predictions of the expected emission regions.

We thank S. Casanova for helpful discussions, acknowledge support from the Research Department of Plasmas with Complex Interactions (Bochum) and from the Lorentz Center, Leiden, The Netherlands. Research on interstellar chemistry at Chalmers has been supported by the Swedish Research Council and the Swedish National Space Board.

REFERENCES

- A. A. Abdo, (Fermi Coll.), et al. *ApJL*, 706:L1, 2009.
- A. A. Abdo, (Fermi Coll.), et al. *ApJ*, 718:348, 2010a.
- A. A. Abdo, (Fermi Coll.), et al. *Science*, 327:1103, 2010b.
- A. A. Abdo, (Fermi Coll.), et al. *ApJ*, 722:1303, 2010c.
- A. A. Abdo, (Fermi Coll.), et al. *ApJ*, 712:459, 2010d.

- J. K. Becker. *Phys. Rep.*, 458:173, 2008.
- A. O. Benz et al. *A & A*, 521:L35, 2010.
- P. L. Biermann et al. *PRL*, 103(6):061101, 2009.
- J. H. Black. *Ch. & Ph. Mol. & Gr. in Sp.*, 109:257, 1998.
- J. H. Black. In *Molecules in Space and Laboratory*, 2007.
- J. H. Black and G. G. Fazio. *ApJL*, 185:L7, 1973.
- P. Blasi et al. *MNRAS*, 361:907, 2005.
- J. M. Brown and A. Carrington. *Rotational Spectroscopy of Diatomic Molecules*. Cambridge Univ. Press, 2003.
- S. Bruderer et al. *A & A*, 521:L44, 2010.
- P. R. Bunker and R. E. Moss. *CPL*, 316(3-4):266, 2000.
- A. D. Critchley et al. *PRL*, 86:1725, 2001.
- A. Dalgarno, M. Yan, and W. Liu. *ApJ Suppl. Series*, 125:237, 1999.
- T. R. Geballe and T. Oka. *ApJL*, 709:L70, 2010.
- M. Gerin et al. *A & A*, 518:L110, 2010.
- M. Goto et al. *ApJ*, 688:306, 2008.
- H. Gupta et al. *A & A*, 521:L47, 2010.
- E. Herbst and W. Klemperer. *ApJ*, 185:505, 1973.
- M. H. Howells and R. A. Kennedy. *CPL*, 184:521, 1991.
- N. Indriolo et al. *ApJ*, 694:257, 2009.
- N. Indriolo et al. *ApJ*, 724:1357, 2010a.
- N. Indriolo et al. *ApJ*, 724:1357, 2010b.
- T. Kamae et al. *ApJ*, 647:692, 2006.
- J. Krelowski et al. *ApJL*, 719:L20, 2010.
- T. Montmerle. *ApJ*, 231:95, 1979.
- T. Montmerle. *ArXiv:0909.0222*, 2009.

- R. E. Moss. *CPL*, 206:83, 1993.
- D. A. Neufeld et al. *A & A*, 521:L10, 2010a.
- D. A. Neufeld et al. *A & A*, 521:L10, 2010b.
- B. Nicholas et al. *MNRAS*, 411:1367, 2011.
- V. Ossenkopf et al. *A & A*, 518:L111, 2010.
- M. Padovani and D. Galli. *A & A*, 530:A109, 2011.
- M. Padovani et al. *A & A*, 501:619, 2009.
- F.-S. Pan and T. Oka. *ApJ*, 305:518, 1986.
- A. G. Posen et al. *Atom D & Nucl D Tab*, 28:265, 1983.
- P. Schilke et al. *A & A*, 521:L11, 2010.
- R. Schlickeiser. *Cosmic Ray Astrophysics*. Springer, 2002.
- A. W. Strong et al. *Ann. Rev. N. Part. Sc.*, 57:285, 2007.
- F. F. S. van der Tak et al. *A & A*, 468:627, 2007.
- F. Wyrowski et al. *A & A*, 521:L34, 2010.